U-Pb Dates for the Nelson and Bayonne Magmatic Suites in the Salmo-Creston Area, Southeastern British Columbia: Tectonic Implications for the Southern Kootenay Arc (Parts of NTS 082F/02, /03, /06, /07)

E.R. Webster, Department of Geoscience, University of Calgary, Calgary, AB, erwebste@ucalgary.ca

D.R.M. Pattison, Department of Geoscience, University of Calgary, Calgary, AB

Webster, E.R. and Pattison, D.R.M. (2014): U-Pb dates for the Nelson and Bayonne magmatic suites in the Salmo-Creston area, southeastern British Columbia: tectonic implications for the southern Kootenay Arc (parts of NTS 082F/02, /03, /06, /07); *in* Geoscience BC Summary of Activities 2013, Geoscience BC, Report 2014-1, p. 99–114.

Introduction

This paper presents new U-Pb zircon dates for igneous intrusions belonging to the Nelson and Bayonne magmatic suites between Creston and Salmo in southeastern British Columbia. This area experienced magmatism, metamorphism and deformation from the Early Jurassic through to the Eocene (Archibald et al., 1983, 1984; Brown et al., 1995; Moynihan and Pattison, 2013; Webster and Pattison, 2013). Determining the age of these intrusions provides constraints on the tectonometamorphic evolution of the area and associated mineralization events.

Regional Geology

The region between Nelson, Salmo and Creston in southeastern BC straddles the tectonic interface between the ancestral North American margin and pericratonic rocks (including Quesnellia) that formed outboard of the margin to the west (Monger et al., 1982; Unterschutz et al., 2002; Figure 1). The accretion and juxtaposition of these rocks occurred during Cordilleran orogenesis from the Early Jurassic through to the Eocene. Three structural domains meet within this area: the Purcell Anticlinorium, the Priest River Complex and the Kootenay Arc (Figure 1). The Purcell Anticlinorium is a large, northerly plunging, Mesozoic fold structure comprising rift-related sedimentary rocks from the Mesoproterozoic Belt-Purcell and Neoproterozoic Windermere supergroups (Price, 2000). The Kootenay Arc occurs on the western flank of the Purcell Anticlinorium and is a narrow arcuate structural feature that is characterized by an increase in metamorphic grade and structural complexity, and a decrease in stratigraphic age compared to the Purcell Anticlinorium (Warren, 1997). The Priest River Complex (PRC) is an Eocene metamorphic core complex that exposes midcrustal rocks and Archean basement. It occurs mainly in Idaho and Washington, but its northerly termination occurs in the study area. The PRC is bounded by two normal fault systems: the west-dipping eastern Newport fault and east-dipping Purcell Trench fault (Rhodes and Hyndman, 1984; Doughty and Price, 1999, 2000; Figure 1).

The bedrock geology of the study area consists primarily of deformed and metamorphosed sedimentary strata. Mesoproterozoic Belt-Purcell Supergroup strata outcrop in the eastern portion of the study area. To the west they are unconformably overlain by the Neoproterozoic Windermere Supergroup (Devlin and Bond, 1988; Warren, 1997; Figure 1). The two supergroups are dominantly composed of clastic, rift-related sedimentary rocks in addition to minor mafic volcanic rocks and sills. Unconformably overlying the Windermere Supergroup, and exposed in the western part of the study area, are early Paleozoic coarse clastic and carbonate rocks.

Numerous granitoid intrusions intrude all of these sedimentary rocks (Figures 2, 3). They range in age from Middle Jurassic to Eocene and are part of larger intrusive suites that extend across southeastern BC (Ghosh, 1995a). Intrusive rocks of the Nelson suite (Nelson batholith, Kuskanax batholith, Bonnington pluton, Trail pluton, Mackie pluton, Mine and Wall stocks) were emplaced between ca. 179 and 159 Ma (Ghosh, 1995a; Evenchick et al., 2007). The rocks of the Nelson intrusive suite are I-type granitoids that range in composition from tonalite to granite (Figure 1; Little, 1960; Ghosh and Lambert, 1995). The Middle Jurassic intrusions typically have staurolite-bearing contact aureoles and were emplaced at depths ranging from 12 to 18 km (Ghent et al., 1991; Pattison and Vogl, 2005). These intrusive suites formed in a magmatic arc, above an east-dipping subduction zone (Ghosh, 1995b).

Quesnel Lake (Figure 1; Quesnel Lake is situated 300 km northwest of Salmon Arm, BC; Logan, 2001). The Bayonne suite is primarily peraluminous, containing two-mica granites with less significant subalkalic granodiorites, aplites and pegmatites (Logan, 2001). Cordierite-bearing

Keywords: *U-Pb LA-MC-ICP-MS, Nelson plutonic suite, Bayonne magmatic suite, Kootenay Arc, Purcell Anticlinorium*

This publication is also available, free of charge, as colour digital files in Adobe Acrobat® PDF format from the Geoscience BC website: http://www.geosciencebc.com/s/DataReleases.asp.

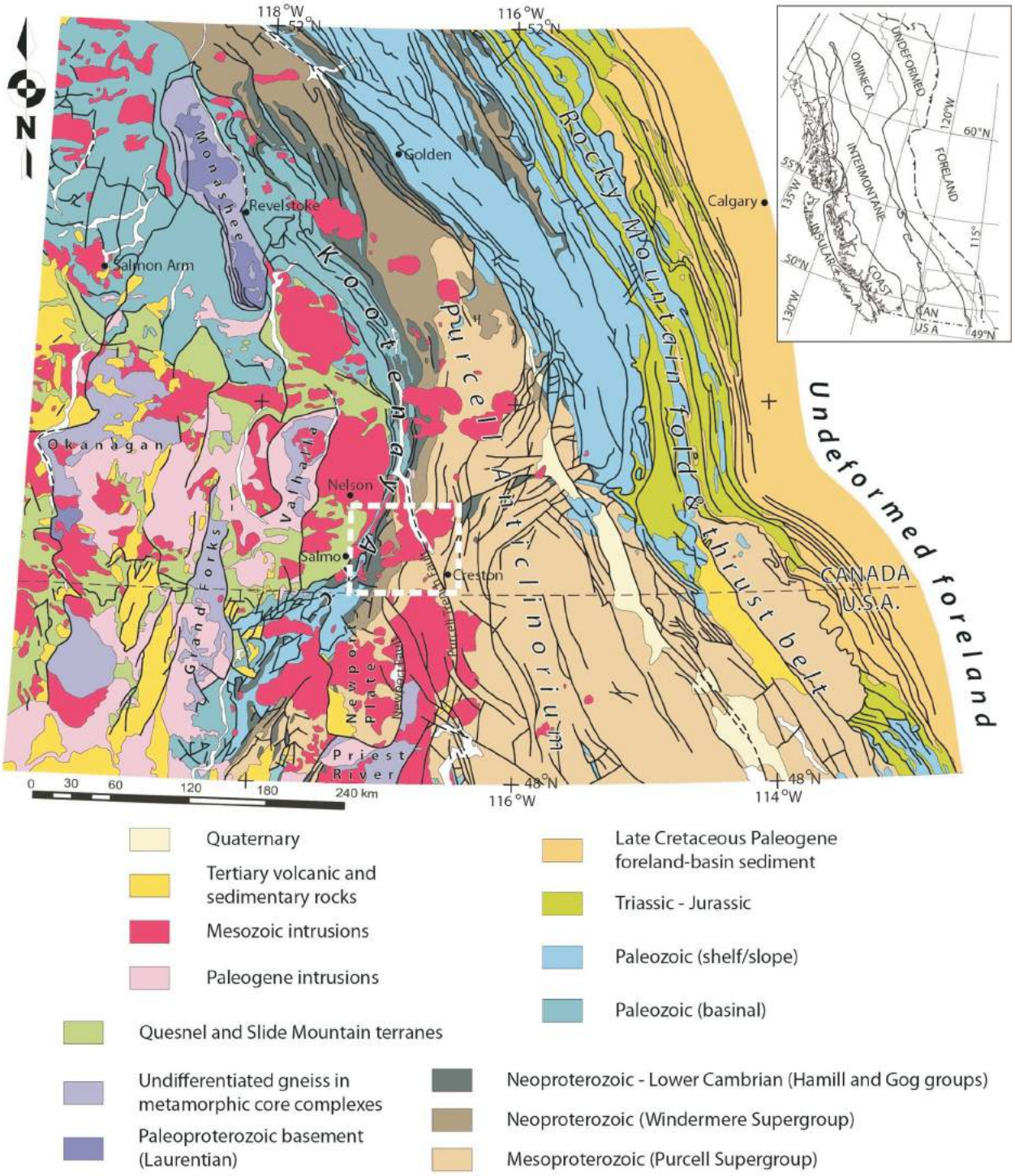

Figure 1. Regional geology of the southeastern Canadian Cordillera. Eocene core complexes are labelled on the map as Priest River, Okanagan, Grand Forks, Monashee and Valhalla. The study area is highlighted by the white dashed square. Map modified from Moynihan and Pattison (2013), originally after Wheeler and McFeely (1991).

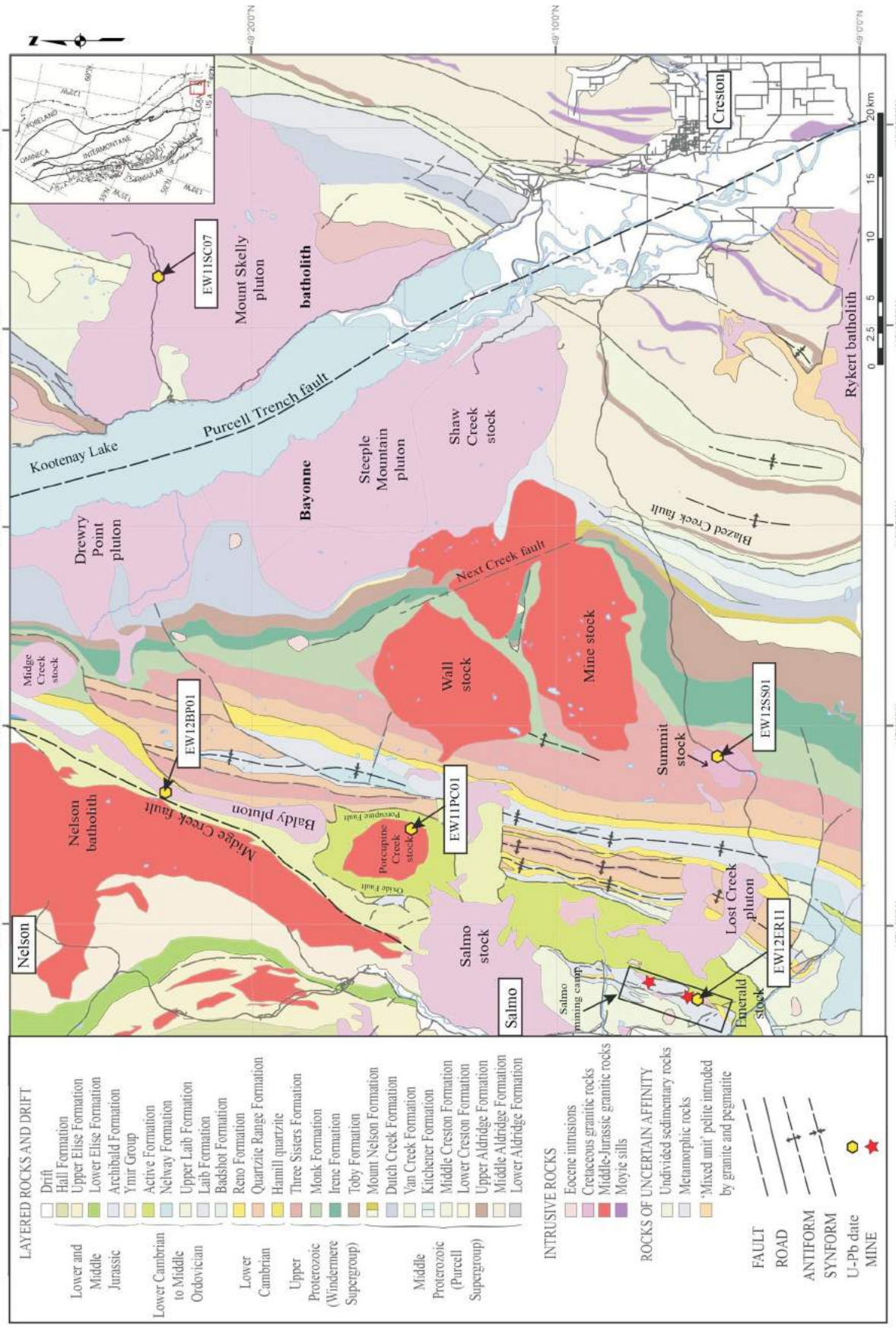

Figure 2. Map showing igneous intrusive bodies within the study area, modified after Webster and Pattison (2013) and compiled from Reesor (1996), Höy and Dunne (1998), Paradis et al. (2009) and Glombick et al. (2010). The Kuskanax batholith, Bonnington pluton, Trail pluton, Mackie pluton are not included on this map. The yellow hexagons represent sample sites used for U-Pb analysis. The two minesites represent the Emerald (south) and Dodger (north) mines of the Salmo mining camp.

contact metamorphic mineral assemblages found adjacent to plutons of the Bayonne suite suggest emplacement depths of less than 12 km (Archibald et al., 1983; Webster and Pattison, 2013). What is referred to as the 'Bayonne batholith' (Figure 2) comprises multiple phases: the Mount Skelly pluton, the Shaw Creek stock, Heather Creek pluton, Drewry Point pluton and Steeple Mountain plutons (Leclair, 1988). Existing geochronology by Davis (1995) and Brown et al. (1999) have shown that individual phases range in age from 99 (Steeple Mountain) to 76 Ma (Shaw Creek).

Description of Granitoid Intrusive Rocks and their Tectonic Setting

Porcupine Creek Stock

The Porcupine Creek stock (PCS) is situated between the tail of the Nelson batholith and the Jurassic Mine and Wall stocks and occupies approximately 15 km^2 (Figures 2, 3). It was emplaced into the Ordovician Active Formation and is bounded on the east and west sides by the Porcupine Creek and Oxide faults, respectively (McAllister, 1951; Einarsen, 1994). The Porcupine Creek fault is a westward-verging thrust fault that dips steeply to the east and strikes north-northeast, and is likely a continuation of the Black Bluff fault. The Oxide fault is an overturned, eastward-verging thrust fault that dips steeply to the east and strikes north-northeast, and is an extension of the Argillite fault to the southwest (Einarsen, 1994).

The PCS has no discernible tectonic fabric and crosscuts regional Jurassic fold structures (Figure 2). The intrusion and its contact aureole also appear to have been unaffected by Cretaceous deformation and Barrovian metamorphism in the footwall of the Midge Creek fault (Webster and Pattison, 2013). The PCS has developed a low pressure (~3.0–3.5 kbar) cordierite-andalusite-biotite contact aureole, similar to the southern part of the Nelson batholith aureole (Pattison and Vogl, 2005).

The sample is composed of a K-feldspar–phyric, biotite-hornblende quartz monzodiorite (Figure 4a). Plagioclase laths and K-feldspar crystals are typically 3–7 mm and form subhedral to anhedral grains. The feldspars are typically intergrown with quartz and the mafic phases, with individual quartz crystals typically <1 mm in size. Abundant biotite and hornblende form ragged crystals up to 2 mm in size. Clinopyroxene crystals are sparse and typically less than 1 mm in diameter. Accessory magnetite and apatite are common, with abundant ~1 mm size titanite crystals. Sericitization of feldspar, and minor alteration of biotite and hornblende to chlorite, is common in this monzodiorite and other intrusive rocks in this study.

Baldy Pluton

The Baldy pluton is an elongate intrusive body that is parallel to the regional structural trend and is situated in the footwall of the Midge Creek fault, adjacent to the tail of the Nelson batholith (Figure 2). It occupies approximately 35 km^2 and was emplaced into regionally metamorphosed Cambrian to Ordovician strata. It formed prior to, or during, penetrative deformation (Leclair et al., 1993). The intrusion is foliated and has a strong mineral lineation that is parallel to those in the adjacent metamorphosed sedimentary rocks. The pluton consists of a coarse-grained, K-feldspar–phyric, biotite-clinopyroxene granodiorite with fine-grained recrystallized quartz, plagioclase and secondary epidote defining a strong lineation. The K-feldspar phenocrysts are locally megacrystic, anhedral and typically have a crystal size between 2 and 5 mm (Figure 4b). Biotite and secondary muscovite crystals are typically 1 mm in size. Accessory magnetite and titanite are common.

Mount Skelly Pluton

The Mount Skelly pluton is the eastern most phase of the Bayonne batholith and occurs on the eastern side of Kootenay Lake, occupying approximately 300 km^2. It is situated in the hangingwall of the Purcell Trench fault (PTF) and has intruded the middle and upper Belt-Purcell Supergroup. The pluton has imparted a low pressure cordierite-andalusite-biotite contact aureole on the surrounding metasedimentary rocks (Webster and Pattison, 2013). The intrusion has no discernible tectonic fabric. The rock sampled is an equigranular, biotite-muscovite granite. The K-feldspar and plagioclase crystals are anhedral to euhedral and are typically 2–5 mm (Figure 4c). Abundant primary biotite and muscovite grains are 1–2 mm and comprise approximately 25% of the rock. Quartz grains are normally <1 mm but some larger grains exist (2–3 mm).

Summit Stock

The Summit Stock is exposed over approximately 5 km^2 at the top of Kootenay Pass (Figure 2) and has intruded into coarse clastic rocks of the Neoproterozoic Three Sisters Formation. This intrusion and the Lost Creek pluton to the west have imparted a low pressure contact aureole on the surrounding low-grade country rocks. The mineral assemblage zonal sequence is cordierite, andalusite±cordierite and sillimanite±K-feldspar (Bjornson, 2012). The contact aureole envelopes both intrusions, with the highest grade mineral assemblages found between them, implying that the two intrusions may be connected at depth. The Summit stock has no tectonic fabric and is a biotite-muscovite granite (Figure 4d). Euhedral to subhedral plagioclase laths are up to 3 mm in size and occasionally show oscillatory zoning. The K-feldspar crystals are subhedral to anhedral and are typically 3–5 mm. Biotite and primary muscovite crystals are euhedral and are typically about 1 mm. Quartz

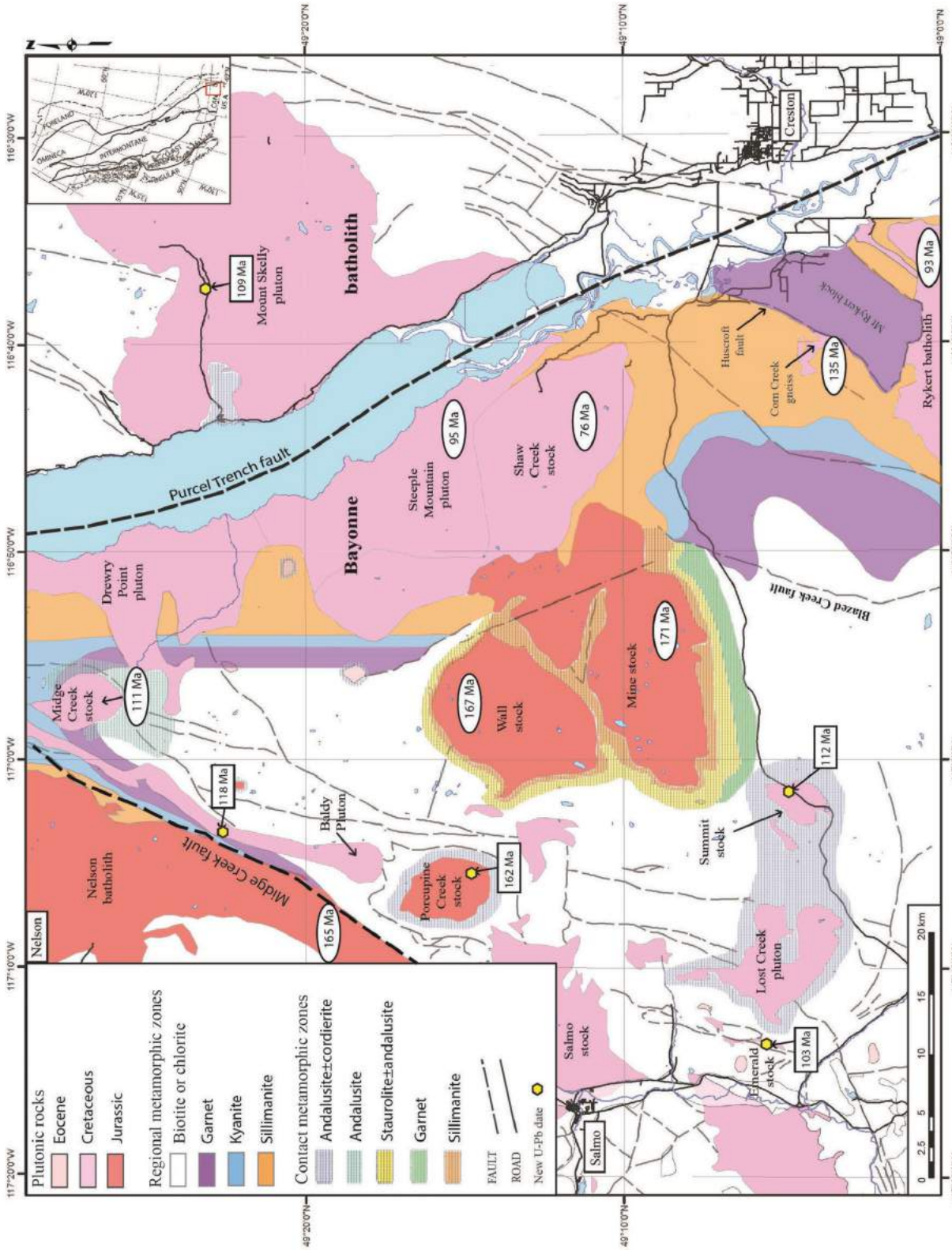

Figure 3. Metamorphic zones and plutonic rocks of the study area, compiled from Glover (1978), Archibald et al. (1983), Leclair (1988), Doughty et al. (1997) and new data. Areas with no shading are of low metamorphic grade. Rectangular boxes are new U-Pb dates from this study and those in oval-shaped boxes are existing ages from previous studies.

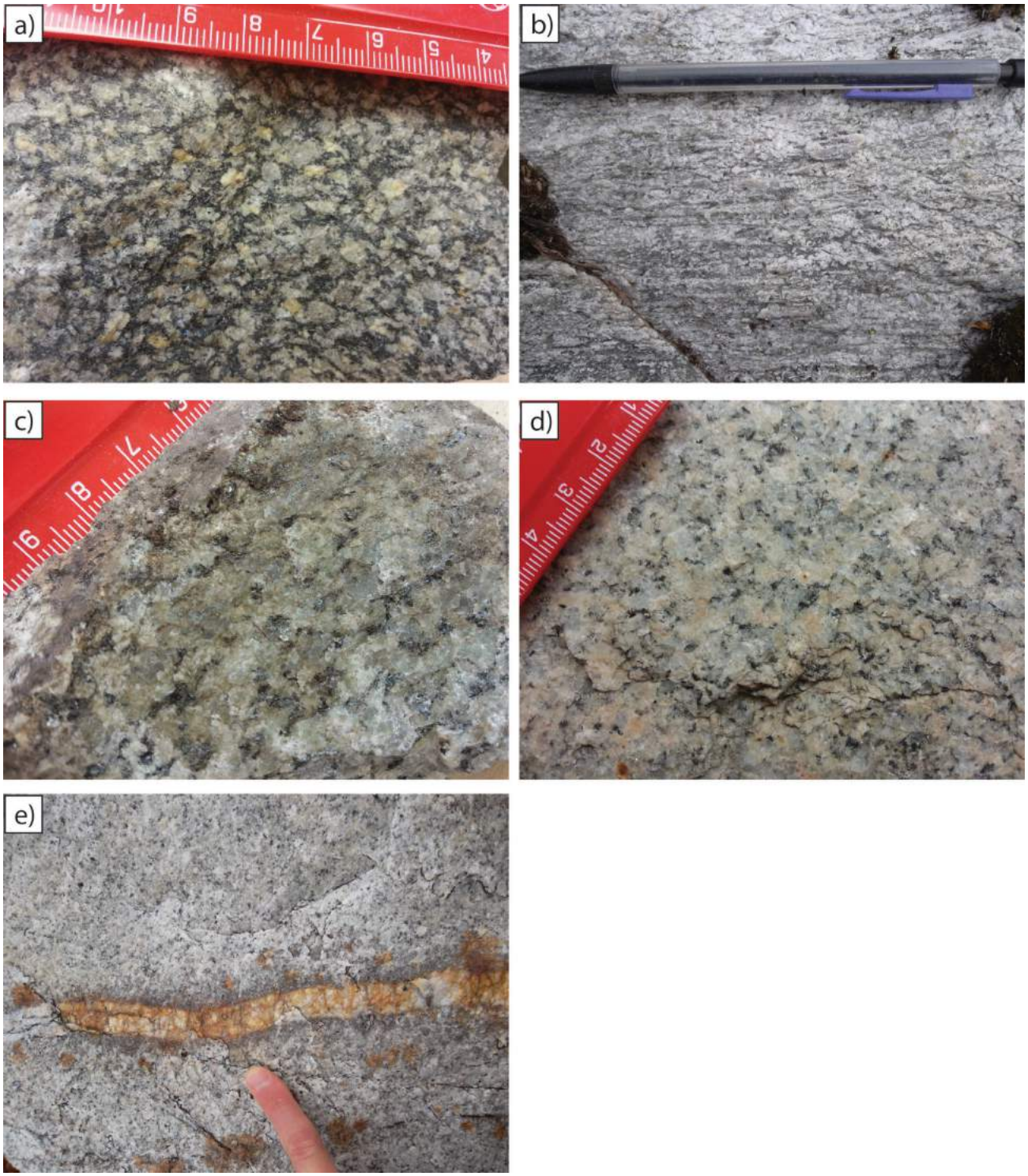

Figure 4. Field pictures of the various igneous intrusive rocks found throughout the study area: **a)** monzodiorite of the Porcupine Creek stock (PCS); **b)** lineated, granodiorite from the Baldy pluton; **c)** two-mica granite of the Mount Skelly pluton; **d)** biotite-muscovite granite of the Summit stock; **e)** biotite granite of the Emerald stock with mineralized quartz vein.

grains are typically 1–2 mm in size. There is accessory magnetite throughout the intrusion.

Emerald Stock

The Emerald Stock crops out over approximately 0.4 km^2 and has intruded into the sedimentary rocks of the Cambrian Laib and Reno formations and also the Ordovician Active Formation, within the historic Salmo mining camp. The carbonate sedimentary rocks (Laib Formation), in contact with the Emerald stock, are typically altered, with rock types ranging from coarse marble to garnet-pyroxene skarn. The skarns are host to Mo-W mineralization, which was mined from the past-producing Emerald and Dodger mines (1.6 million tons grading 0.76% W, Giroux and Grunenberg, 2009; Figure 2). The intrusion is an undeformed, equigranular biotite-granite. Plagioclase and K-feldspar crystals are subhedral to anhedral and are typically about 1 mm (Figure 4e). Biotite phenocrysts are ragged and typically 2–3 mm in diameter, although they have been almost completely replaced by chlorite, with secondary rutile. Accessory magnetite occurs throughout the intrusion.

Analytical Techniques

One sample from each intrusion was collected for U-Pb zircon isotopic age dating at the Radiogenic Isotope Facility (RIF) in the Department of Earth and Atmospheric Sciences, at the University of Alberta. Zircon grains were separated from samples using standard magnetic and heavy liquid separation techniques at the Apatite to Zircon Inc. laboratories (Viola, Idaho). The zircon separates were mounted in 1 cm^2 epoxy pucks that were subsequently ground down to expose the internal structure of the zircon, before being polished for analysis. The pucks were washed in 5.5M HNO_3 at 21°C for 20 seconds to minimize surface Pb contamination.

Prior to U-Pb dating, cathodoluminescence (CL) images were obtained using a Gatan MonoCL4 Elite detector attached to a FEI Quanta 250 FEG field emission scanning electron microscope at the Department of Geoscience, University of Calgary. Laser-ablation inductively coupled plasma–mass spectrometry (LA-ICP-MS) analyses were acquired with a New Wave UP-213 Nd:YAG laser ablation system in conjunction with a Nu Plasma multiple-collector, inductively coupled plasma–mass spectrometry (MC-ICP-MS) instrument. The latter is equipped with a collector block including 12 Faraday collectors and 3 ion counters (Simonetti et al., 2005) allowing static collection of both U and Pb isotopes. The laser diameter was 30 μm with a laser frequency of 4 Hz and ~3 J/cm^2 energy density. Data were collected over a 30 second cycle in 1 second increments. An in-house monazite standard from Madagascar with a $^{206}Pb/^{238}U$ age of 517.9 Ma was used as a primary calibration reference. This has been dated by isotope dilution–thermal ionization mass spectrometry (ID-TIMS; Heaman, unpublished data) and is the same as that used by Simonetti et al. (2006).

Results

The U-Pb isotopic data are shown in Table 1 for five plutonic rocks from the study area. Isotopic ratios are uncorrected for common Pb, and errors are reported at the 2σ level. Inherited cores were observed in all five samples and they consistently yielded older dates that hindered the determination of the crystallization age (Figure 5). As a result of this common feature, multiple analyses were excluded from each sample. Analyses containing high common Pb values, highly discordant ages and obvious outliers were discarded. After data reduction, weighted mean $^{206}Pb/^{238}U$ ages and Tera-Wasserburg U-Pb concordia plots (Tera and Wasserburg, 1972) were calculated using Isoplot v. 3.0 (Ludwig, 2003).

Porcupine Creek Stock

Sample EW11PC01 from the Porcupine Creek stock contains zircon grains that are typically euhedral, prismatic and 50–100 μm long (Figure 5a). The grains display well-developed oscillatory zoning, with some grains displaying a complex internal structure that is possibly inherited or detrital in origin. The cores yielded significantly older ages and were disregarded from future consideration. Twenty-six analyses from 25 zircon grains yielded an average $^{206}Pb/^{238}U$ age of 162.6 ±1.3 Ma (Mean Square Weighted Deviation, MSWD = 1.15), interpreted to be the age of crystallization (Figure 5c).

Baldy Pluton

Sample EW12BP01 from the Baldy Pluton contains zircon grains that are euhedral, prismatic and typically 75–100 μm in length (Figure 5b). The crystals have well-developed oscillatory zoning and resorbed, anhedral cores with complex internal structures (Figure 5b). Four spots ablated through the well-zoned rim and likely partly analyzed the complex internal core, yielding significantly older ages. These analyses were excluded from the calculations. Twenty-five analyses from 23 zircon grains yielded an average $^{206}Pb/^{238}U$ age of 117.5 ±1.3 Ma (MSWD = 1.13; Figure 5d).

Mount Skelly Pluton

Sample EW11SC07 from the Mount Skelly pluton of the Bayonne batholith contains zircon grains that are typically euhedral to subhedral, with the latter showing evidence of partial resorption (25–75 μm long; Figure 6a). Most of the grains display oscillatory zoning and have complex, resorbed, internal cores. As a result of the smaller size

Table 1. U-Pb zircon isotopic data for five granitic rocks from the study area. Data was acquired using laser-ablation, multiple-collector, inductively coupled plasma–mass spectrometry.

Sample number	^{206}Pb (cps)	^{204}Pb (cps)	Isotopic ratios							^{207}Pb^{1}/^{206}Pb^{1}	2σ	^{207}Pb^{1}/^{235}U	2σ	^{206}Pb^{1}/^{238}U	2σ
			^{207}Pb/^{206}Pb	2σ	^{207}Pb/^{235}U	2σ	^{206}Pb/^{238}U	2σ	ρ	age (Ma)	error (Ma)	age (Ma)	error (Ma)	age (Ma)	error (Ma)
EW11PC01-1A	154132	598	0.0501	0.0014	0.1746	0.0095	0.0253	0.0012	0.866	199	62	163	8	161	7
EW11PC01-1B	136407	519	0.0500	0.0014	0.1784	0.0086	0.0259	0.0010	0.802	195	66	167	7	165	6
EW11PC01-2	173623	892	0.0510	0.0016	0.1871	0.0135	0.0266	0.0017	0.898	241	72	174	12	169	11
EW11PC01-3	427013	454	0.0494	0.0013	0.1706	0.0080	0.0250	0.0010	0.816	167	62	160	7	159	6
EW11PC01-4	161852	360	0.0494	0.0014	0.1780	0.0095	0.0261	0.0012	0.853	168	64	166	8	166	7
EW11PC01-5	98764	369	0.0505	0.0017	0.1754	0.0091	0.0252	0.0010	0.767	220	75	164	8	160	6
EW11PC01-8	143546	267	0.0487	0.0015	0.1646	0.0084	0.0245	0.0010	0.811	136	69	155	7	156	6
EW11PC01-9	196342	388	0.0507	0.0015	0.1741	0.0088	0.0249	0.0010	0.808	226	68	163	8	159	6
EW11PC01-10	156744	338	0.0485	0.0013	0.1664	0.0085	0.0249	0.0011	0.843	126	64	156	7	158	7
EW11PC01-11	159662	284	0.0492	0.0014	0.1687	0.0082	0.0248	0.0010	0.813	159	65	158	7	158	6
EW11PC01-12	699219	209	0.0867	0.0025	0.9601	0.0874	0.0803	0.0069	0.948	1354	55	683	44	498	41
EW11PC01-13	147836	682	0.0519	0.0015	0.1775	0.0090	0.0248	0.0010	0.828	281	64	166	8	158	7
EW11PC01-14	155172	738	0.0529	0.0016	0.1916	0.0098	0.0262	0.0011	0.810	327	67	178	8	167	7
EW11PC01-15	146591	811	0.0515	0.0014	0.1871	0.0092	0.0264	0.0011	0.826	263	62	174	8	168	7
EW11PC01-16	219504	668	0.0510	0.0014	0.1829	0.0090	0.0260	0.0010	0.822	243	63	171	8	165	7
EW11PC01-17	148349	637	0.0508	0.0014	0.1826	0.0096	0.0261	0.0012	0.853	233	62	170	8	166	7
EW11PC01-18	137889	870	0.0622	0.0035	0.2264	0.0155	0.0264	0.0010	0.559	680	117	207	13	168	6
EW11PC01-19	186897	508	0.0500	0.0014	0.1753	0.0089	0.0254	0.0011	0.845	196	62	164	8	162	7
EW11PC01-20	143891	517	0.0516	0.0014	0.1826	0.0084	0.0257	0.0009	0.799	266	62	170	7	163	6
EW11PC01-21	174064	432	0.0500	0.0013	0.1761	0.0097	0.0256	0.0012	0.870	193	62	165	8	163	8
EW11PC01-22	107698	495	0.0507	0.0014	0.1776	0.0082	0.0254	0.0010	0.806	228	62	166	7	162	6
EW11PC01-23	143644	526	0.0534	0.0017	0.1929	0.0108	0.0262	0.0012	0.823	345	71	179	9	167	8
EW11PC01-24	173808	304	0.0507	0.0014	0.1771	0.0080	0.0253	0.0009	0.781	227	64	166	7	161	6
EW11PC01-25	171321	313	0.0492	0.0013	0.1699	0.0073	0.0251	0.0008	0.778	156	62	159	6	160	5
EW11PC01-26	153332	391	0.0505	0.0014	0.1808	0.0079	0.0259	0.0009	0.773	219	63	169	7	165	5
EW11PC01-27	158112	456	0.0505	0.0014	0.1808	0.0084	0.0260	0.0010	0.795	218	64	169	7	165	6
EW11PC01-28	254688	400	0.0548	0.0027	0.2157	0.0194	0.0286	0.0022	0.839	403	106	198	16	182	13
EW11PC01-29	197674	379	0.0490	0.0013	0.1706	0.0074	0.0253	0.0009	0.777	146	63	160	6	161	5
EW11PC01-30	196760	393	0.0499	0.0014	0.1769	0.0067	0.0257	0.0006	0.662	188	64	165	6	164	4
EW12BP01-1	342874	850	0.0489	0.0008	0.1276	0.0067	0.0189	0.0010	0.955	143	36	122	6	121	6
EW12BP01-2	147126	695	0.0498	0.0009	0.1206	0.0063	0.0175	0.0009	0.944	188	39	116	6	112	5
EW12LBP01-3B	190442	680	0.0488	0.0008	0.1274	0.0073	0.0189	0.0010	0.960	139	38	122	7	121	7
EW12BP01-3	127623	754	0.0494	0.0009	0.1295	0.0091	0.0190	0.0013	0.967	165	41	124	8	122	8
EW12BP01-4	239506	680	0.0486	0.0008	0.1203	0.0062	0.0179	0.0009	0.952	130	37	115	6	115	6
EW12BP01-6	252352	683	0.0554	0.0015	0.1994	0.0158	0.0261	0.0020	0.944	427	57	185	13	166	12
EW12BP01-7	1451648	684	0.0940	0.0043	1.8414	0.4778	0.1420	0.0363	0.984	1509	85	1060	158	856	202
EW12BP01-8	597700	718	0.0798	0.0055	0.8428	0.1855	0.0766	0.0160	0.950	1191	130	621	97	476	95
EW12BP01-9	581938	1032	0.0556	0.0015	0.1384	0.0084	0.0180	0.0010	0.898	438	58	132	7	115	6
EW12BP01-10	257809	699	0.0484	0.0008	0.1228	0.0060	0.0184	0.0008	0.943	119	38	118	5	118	5
EW12BP01-11	338820	671	0.0484	0.0007	0.1183	0.0064	0.0177	0.0009	0.959	118	36	114	6	113	6
EW12BP01-12	317908	622	0.0509	0.0013	0.1277	0.0094	0.0182	0.0013	0.939	238	57	122	8	116	8
EW12BP01-13	329196	722	0.0494	0.0008	0.1263	0.0065	0.0186	0.0009	0.950	165	37	121	6	119	6
EW12BP01-14	323267	687	0.0487	0.0008	0.1256	0.0085	0.0187	0.0012	0.970	133	38	120	8	119	8
EW12BP01-15	362643	609	0.0480	0.0008	0.1260	0.0062	0.0190	0.0009	0.947	99	37	120	6	122	6
EW12BP01-16	229035	600	0.0483	0.0008	0.1168	0.0105	0.0175	0.0016	0.982	113	40	112	10	112	10
EW12BP01-17	290212	651	0.0485	0.0008	0.1248	0.0060	0.0187	0.0008	0.941	124	38	119	5	119	5
EW12BP01-17B	354986	632	0.0483	0.0008	0.1208	0.0060	0.0182	0.0009	0.946	113	38	116	5	116	5
EW12BP01-18	246695	609	0.0481	0.0008	0.1257	0.0065	0.0189	0.0009	0.951	105	37	120	6	121	6

Table 1 (continued)

Sample number	^{206}Pb (cps)	^{204}Pb (cps)	Isotopic ratios							$^{207}Pb^{1}/^{206}Pb^{1}$ age (Ma)	2σ error (Ma)	$^{207}Pb^{1}/^{235}U$ age (Ma)	2σ error (Ma)	$^{206}Pb^{1}/^{238}U$ age (Ma)	2σ error (Ma)
			$^{207}Pb/^{206}Pb$	2σ	$^{207}Pb/^{235}U$	2σ	$^{206}Pb/^{238}U$	2σ	ρ						
EW12BP01-19	39778	544	0.0506	0.0017	0.1261	0.0071	0.0181	0.0008	0.799	220	76	121	6	116	5
EW12BP01-20	129426	536	0.0495	0.0010	0.1225	0.0059	0.0179	0.0008	0.909	174	46	117	5	115	5
EW12BP01-21	298525	575	0.0487	0.0008	0.1246	0.0066	0.0185	0.0009	0.948	136	39	119	6	118	6
EW12BP01-22	169034	482	0.0492	0.0012	0.1189	0.0069	0.0175	0.0009	0.907	160	56	114	6	112	6
EW12BP01-23	293664	479	0.0486	0.0008	0.1225	0.0062	0.0183	0.0009	0.949	126	37	117	6	117	6
EW12BP01-24	269535	528	0.0499	0.0009	0.1307	0.0066	0.0190	0.0009	0.933	193	42	125	6	121	6
EW12BP01-26	223998	515	0.0488	0.0008	0.1270	0.0065	0.0189	0.0009	0.946	136	39	121	6	121	6
EW12BP01-27	3226855	662	0.0988	0.0015	2.5223	0.1313	0.1852	0.0092	0.955	1601	28	1278	37	1095	50
EW12BP01-28	381725	592	0.0480	0.0008	0.1259	0.0071	0.0190	0.0010	0.955	98	39	120	6	122	6
EW12BP01-30	435674	554	0.0486	0.0008	0.1252	0.0064	0.0187	0.0009	0.947	130	38	120	6	119	6
EW11SC07-1	553055	318	0.0553	0.0017	0.1543	0.0113	0.0202	0.0013	0.905	423	68	146	10	129	8
EW11SC07-2	1222072	52	0.0987	0.0039	1.7887	0.4079	0.1314	0.0295	0.985	1600	73	1041	139	796	166
EW11SC07-3	439729	42	0.0476	0.0013	0.1137	0.0054	0.0173	0.0007	0.831	80	62	109	5	111	4
EW11SC07-5	345152	542	0.0573	0.0017	0.1735	0.0090	0.0220	0.0009	0.808	503	66	162	8	140	6
EW11SC07-6	197464	570	0.0557	0.0019	0.1482	0.0087	0.0193	0.0009	0.817	440	73	140	8	123	6
EW11SC07-8	613081	436	0.0719	0.0035	0.3600	0.0481	0.0363	0.0045	0.931	984	96	312	35	230	28
EW11SC07-9	530693	494	0.0484	0.0013	0.1105	0.0047	0.0166	0.0005	0.777	117	62	106	4	106	3
EW11SC07-10	519694	386	0.0789	0.0062	1.0720	0.3031	0.0985	0.0267	0.960	1171	149	740	139	606	155
EW11SC07-11	491507	332	0.0594	0.0038	0.1933	0.0293	0.0236	0.0032	0.907	581	133	179	25	150	20
EW11SC07-13	545551	376	0.0488	0.0013	0.1127	0.0052	0.0168	0.0006	0.811	138	62	108	5	107	4
EW11SC07-15	581477	602	0.0513	0.0016	0.1218	0.0051	0.0172	0.0005	0.668	255	70	117	5	110	3
EW11SC07-18	435449	383	0.0554	0.0028	0.1415	0.0115	0.0185	0.0012	0.779	429	110	134	10	118	7
EW11SC07-19	594387	271	0.0609	0.0036	0.1970	0.0281	0.0235	0.0030	0.912	636	121	183	24	149	19
EW11SC07-26	309287	225	0.0488	0.0013	0.1183	0.0055	0.0176	0.0007	0.813	139	62	113	5	112	4
EW11SC07-27	611177	253	0.0485	0.0013	0.1105	0.0048	0.0165	0.0006	0.789	124	61	106	4	106	4
EW11SC07-27B	772281	200	0.0478	0.0013	0.1085	0.0043	0.0164	0.0005	0.743	91	62	105	4	105	3
EW11SC07-34	574207	446	0.0479	0.0013	0.1138	0.0047	0.0172	0.0006	0.772	94	62	109	4	110	4
EW11SC07-35	929693	506	0.0761	0.0022	0.8093	0.0561	0.0771	0.0049	0.910	1097	56	602	31	479	29
EW11SC07-36	159564	166	0.0486	0.0013	0.1178	0.0052	0.0176	0.0006	0.788	127	63	113	5	112	4
EW11SC07-37B	572510	216	0.0516	0.0016	0.1231	0.0112	0.0173	0.0015	0.936	266	71	118	10	111	9
EW11SC07-39	621565	218	0.0630	0.0019	0.2133	0.0084	0.0246	0.0006	0.658	708	62	196	7	156	4
EW11SC07-40	457085	211	0.0478	0.0013	0.1111	0.0049	0.0169	0.0006	0.801	87	62	107	4	108	4
EW11SC07-41	812426	321	0.0478	0.0013	0.1117	0.0047	0.0169	0.0005	0.773	90	62	108	4	108	3
EW11SC07-42	183276	238	0.0475	0.0013	0.1119	0.0048	0.0171	0.0006	0.782	72	63	108	4	109	4
EW11SC07-43	594015	276	0.0491	0.0014	0.1182	0.0052	0.0175	0.0006	0.764	154	65	113	5	112	4
EW11SC07-44	738853	257	0.0479	0.0013	0.1146	0.0053	0.0173	0.0007	0.822	96	62	110	5	111	4
EW11SC07-45	449615	150	0.0477	0.0013	0.1124	0.0052	0.0171	0.0006	0.817	86	62	108	5	109	4
EW11SC07-46	630513	159	0.0478	0.0013	0.1116	0.0051	0.0169	0.0006	0.814	88	62	107	5	108	4
EW12SS01-1	110074	461	0.0487	0.0006	0.1154	0.0048	0.0172	0.0007	0.951	135	30	111	4	110	4
EW12SS01-2	156073	418	0.0491	0.0006	0.1214	0.0059	0.0179	0.0008	0.968	151	29	116	5	115	5
EW12SS01-3	127935	418	0.0490	0.0006	0.1171	0.0043	0.0173	0.0006	0.940	149	29	112	4	111	4
EW12SS01-4	360149	369	0.0481	0.0005	0.1183	0.0044	0.0179	0.0006	0.959	103	24	114	4	114	4
EW12SS01-5	252120	409	0.0483	0.0005	0.1129	0.0052	0.0170	0.0008	0.972	112	25	109	5	108	5
EW12SS01-6	355400	331	0.0488	0.0007	0.1139	0.0047	0.0169	0.0007	0.938	138	33	110	4	108	4
EW12SS01-7	313877	320	0.0479	0.0005	0.1156	0.0050	0.0175	0.0007	0.967	94	26	111	5	112	5
EW12SS01-8	66232	277	0.0471	0.0008	0.1129	0.0051	0.0174	0.0007	0.925	55	40	109	5	111	5
EW12SS01-9	172338	255	0.0481	0.0007	0.1168	0.0050	0.0176	0.0007	0.948	105	32	112	5	113	5
EW12SS01-10	343860	311	0.0482	0.0005	0.1163	0.0052	0.0175	0.0008	0.971	109	25	112	5	112	5

Table 1 (continued)

Sample number	^{206}Pb (cps)	^{204}Pb (cps)	Isotopic ratios							$^{207}Pb^{1}/^{206}Pb^{1}$ age (Ma)	2σ error (Ma)	$^{207}Pb^{1}/^{235}U$ age (Ma)	2σ error (Ma)	$^{206}Pb^{1}/^{238}U$ age (Ma)	2σ error (Ma)
			$^{207}Pb/^{206}Pb$	2σ	$^{207}Pb/^{235}U$	2σ	$^{206}Pb/^{238}U$	2σ	ρ						
EW12SS01-11	420076	283	0.0482	0.0005	0.1161	0.0056	0.0175	0.0008	0.974	107	25	112	5	112	5
EW12SS01-12	130685	248	0.0482	0.0006	0.1157	0.0067	0.0174	0.0010	0.978	110	29	111	6	111	6
EW12SS01-13	600286	316	0.0479	0.0005	0.1178	0.0048	0.0178	0.0007	0.965	97	25	113	4	114	4
EW12SS01-14	56963	287	0.0494	0.0013	0.1169	0.0059	0.0172	0.0007	0.864	167	58	112	5	110	5
EW12SS01-15	163014	255	0.0481	0.0007	0.1186	0.0047	0.0179	0.0007	0.938	104	32	114	4	114	4
EW12SS01-16	148142	318	0.0497	0.0008	0.1202	0.0053	0.0175	0.0007	0.930	181	37	115	5	112	5
EW12SS01-17	100994	399	0.0499	0.0008	0.1193	0.0052	0.0173	0.0007	0.935	192	36	114	5	111	4
EW12SS01-18	235442	366	0.0535	0.0032	0.1286	0.0115	0.0174	0.0011	0.735	348	131	123	10	111	7
EW12SS01-19	34807	385	0.0549	0.0022	0.1311	0.0077	0.0173	0.0007	0.728	410	88	125	7	111	5
EW12SS01-20	161616	419	0.0489	0.0006	0.1172	0.0049	0.0174	0.0007	0.961	142	27	113	4	111	4
EW12SS01-21	1043904	453	0.0483	0.0005	0.1170	0.0055	0.0176	0.0008	0.971	114	26	112	5	112	5
EW12SS01-22	867949	421	0.1077	0.0011	4.9656	0.2274	0.3345	0.0149	0.975	1760	18	1813	38	1860	72
EW12SS01-22B	525409	427	0.1064	0.0032	4.8173	0.3798	0.3285	0.0239	0.923	1738	55	1788	64	1831	115
EW12SS01-23	66602	423	0.0514	0.0013	0.1229	0.0060	0.0174	0.0007	0.844	257	59	118	5	111	5
EW12SS01-24	258631	447	0.0487	0.0005	0.1185	0.0053	0.0177	0.0008	0.969	133	26	114	5	113	5
EW12SS01-25	91785	347	0.0488	0.0007	0.1179	0.0059	0.0175	0.0008	0.953	137	35	113	5	112	5
EW12SS01-26	880697	375	0.0481	0.0005	0.1172	0.0045	0.0177	0.0007	0.961	103	25	113	4	113	4
EW12SS01-27	883260	323	0.0478	0.0005	0.1185	0.0043	0.0180	0.0006	0.959	90	24	114	4	115	4
EW12SS01-28	234529	272	0.0480	0.0006	0.1159	0.0086	0.0175	0.0013	0.985	99	30	111	8	112	8
EW12SS01-29	453932	245	0.0480	0.0005	0.1163	0.0047	0.0176	0.0007	0.964	98	25	112	4	112	4
EW13ER11-1	256432	565	0.0506	0.0009	0.1119	0.0057	0.0160	0.0008	0.944	224	39	108	5	103	5
EW13ER11-2	176365	511	0.0525	0.0010	0.1823	0.0167	0.0252	0.0022	0.976	309	45	170	14	160	14
EW13ER11-4	31488	342	0.0465	0.0010	0.1019	0.0055	0.0159	0.0008	0.911	26	52	99	5	102	5
EW13ER11-4B	43936	260	0.0461	0.0008	0.1017	0.0054	0.0160	0.0008	0.938	4	44	98	5	102	5
EW13ER11-6	84705	373	0.0520	0.0016	0.1155	0.0067	0.0161	0.0008	0.850	283	69	111	6	103	5
EW13ER11-7	137683	328	0.0472	0.0008	0.1121	0.0061	0.0172	0.0009	0.947	59	41	108	6	110	6
EW13ER11-8	29751	306	0.0470	0.0019	0.1066	0.0070	0.0164	0.0008	0.781	50	95	103	6	105	5
EW13ER11-9	164354	519	0.0506	0.0014	0.1147	0.0062	0.0164	0.0008	0.860	224	63	110	6	105	5
EW13ER11-10	315584	559	0.0553	0.0013	0.1032	0.0056	0.0135	0.0007	0.907	424	51	100	5	87	4
EW12ER11-11	598715	1180	0.0550	0.0025	0.0827	0.0059	0.0109	0.0006	0.776	413	98	81	6	70	4
EW12ER11-12	179680	919	0.0612	0.0028	0.1333	0.0086	0.0158	0.0007	0.700	647	96	127	8	101	5
EW12ER11-13	260021	861	0.0488	0.0008	0.1100	0.0057	0.0163	0.0008	0.950	140	38	106	5	104	5
EW12ER11-14	143686	763	0.0487	0.0008	0.1096	0.0057	0.0163	0.0008	0.950	132	38	106	5	104	5
EW12ER11-15	272119	792	0.1064	0.0033	2.6289	0.4975	0.1793	0.0335	0.986	1738	56	1309	130	1063	180
EW12ER11-16	139390	748	0.0486	0.0008	0.1065	0.0051	0.0159	0.0007	0.931	131	40	103	5	102	4
EW12ER11-18	338499	714	0.0495	0.0008	0.0986	0.0057	0.0145	0.0008	0.959	170	38	95	5	93	5
EW12ER11-19	163182	693	0.0495	0.0014	0.1005	0.0057	0.0147	0.0007	0.866	172	65	97	5	94	5
EW12ER11-19B	99005	734	0.0493	0.0009	0.1020	0.0050	0.0150	0.0007	0.935	163	40	99	5	96	4
EW12ER11-21	66183	687	0.0496	0.0010	0.1130	0.0059	0.0165	0.0008	0.930	178	44	109	5	106	5
EW12ER11-22	96857	600	0.0491	0.0009	0.1126	0.0057	0.0166	0.0008	0.933	152	42	108	5	106	5
EW12ER11-25	325856	837	0.0599	0.0021	0.1086	0.0074	0.0132	0.0008	0.852	599	75	105	7	84	5
EW12ER11-26	162347	520	0.0481	0.0009	0.1108	0.0053	0.0167	0.0007	0.918	103	45	107	5	107	5
EW12ER11-31	520703	726	0.0482	0.0007	0.1039	0.0051	0.0156	0.0007	0.948	109	36	100	5	100	5
EW12ER11-32	604139	683	0.0484	0.0008	0.1007	0.0050	0.0151	0.0007	0.939	118	39	97	5	97	4
EW12ER11-33	132001	678	0.0492	0.0012	0.1063	0.0060	0.0157	0.0008	0.899	155	57	103	6	100	5

[1]Radiogenic Pb

Abbreviations: cps, counts per second

range and large internal detrital cores, 13 spots were excluded from the calculations. Fifteen spot analyses from 14 zircon grains produced an average $^{206}Pb/^{238}U$ age of 108.8 ±1.2 Ma (MSWD = 1.5; Figure 6c).

Summit Stock

Zircon crystals from sample EW12SS01, taken from the Summit stock, are typically anhedral, display well-developed oscillatory zoning and fall in the size range 50–100 µm long (Figure 6b). The majority of the zircon crystals have complex, resorbed cores that appear bright in the CL images. Six spots yielded significantly older ages and were excluded from the calculations. Twenty-three analyses from 23 zircon grains produced an average $^{206}Pb/^{238}U$ age of 111.83 ±0.86 Ma (MSWD = 0.58; Figure 6d).

Emerald Stock

Sample EW12ER11 from the Emerald stock yielded anhedral zircon grains that display well-developed oscillatory zoning and are typically 50–100 µm in length (Figure 6e). Seven spots yielded significantly older cores and were removed from the calculations. Seventeen analyses from 16 zircon grains yielded an average $^{206}Pb/^{238}U$ age of 101.7 ±2.2 Ma (MSWD = 3.5; Figure 6f). The large MSWD of 3.5 indicates there are likely two populations of zircons. This may be the result of a prolonged crystallization period or multiple pulses of magmatism.

Discussion

The five new zircon U-Pb dates, from granitic intrusive rocks in the Creston-Salmo area, provide improved age

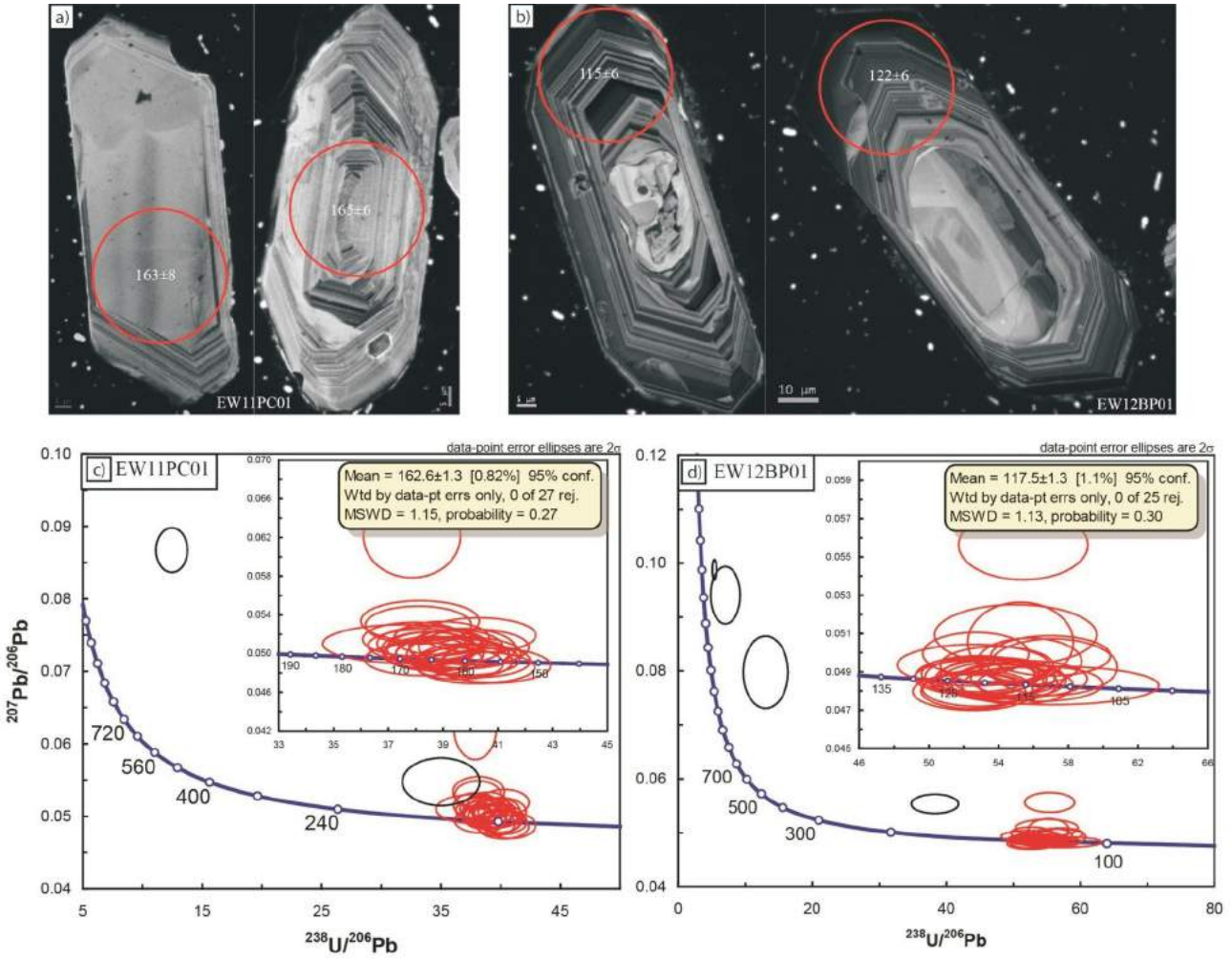

Figure 5. a) Cathodoluminescence images of select zircon grains from the Porcupine Creek stock. The red circles represent the location of the laser spot when acquiring analysis. The associated values are the $^{206}Pb/^{238}U$ ages and corresponding 2σ errors. **b)** Cathodoluminescence images of select zircon grains from the Baldy pluton. **c)** Tera-Wasserburg U-Pb concordia plot for sample EW11PC01. The analyses corresponding to the red error ellipses were used in determining a date for the intrusion, the black error ellipses were discarded. This is the same for all of the Tera-Wasserburg U-Pb concordia plots. **d)** Tera-Wasserburg U-Pb concordia plot for sample EW12BP01.

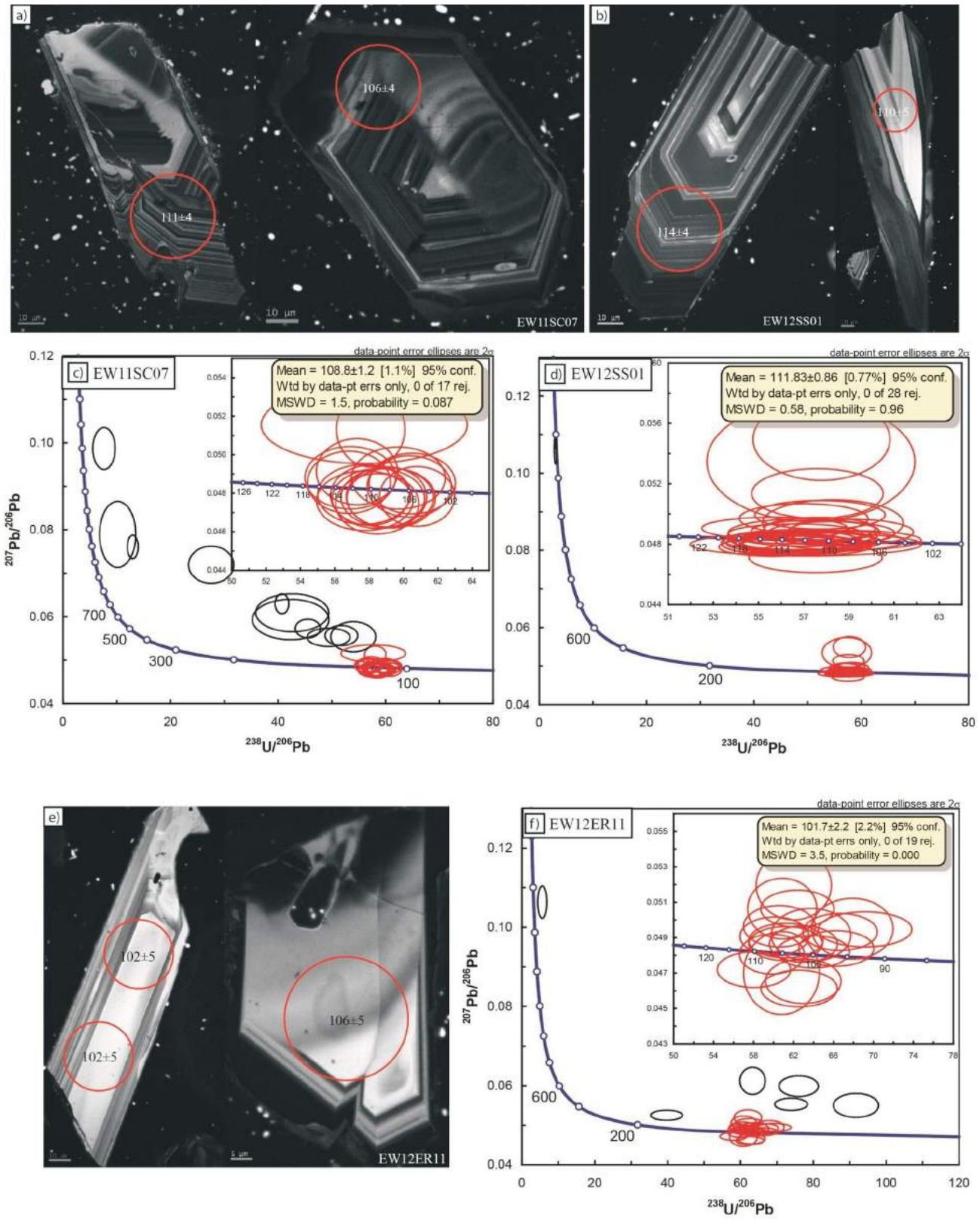

Figure 6. a) Cathodoluminescence images of select zircon grains from the Mount Skelly pluton. The red circles represent the location of the laser spot when acquiring analysis. The associated values are the $^{206}Pb/^{238}U$ ages and corresponding 2σ errors. **b)** Cathodoluminescence images of select zircon grains from the Summit stock. **c)** Tera-Wasserburg U-Pb concordia plot for sample EW11SC07. **d)** Tera-Wasserburg U-Pb concordia plot for sample EW12SS01. **e)** Cathodoluminescence images of select zircon grains from the Emerald stock. **f)** Tera-Wasserburg U-Pb concordia plot for sample EW12ER11.

constraints for magmatism and deformation in this region of southeastern BC. The U-Pb zircon date of 162.6 ±1.3 Ma for the Porcupine Creek stock is interpreted as the crystallization age. Ages obtained by Ghosh (1995a) for the nearby Nelson plutonic suite (172–161 Ma) overlap with this age, suggesting the Porcupine Creek stock is part of the Nelson suite.

The low pressure cordierite and andalusite contact aureole, adjacent to the Porcupine Creek stock (163 Ma), formed at a lower pressure than the staurolite-bearing contact aureole around the older (171 and 167 Ma) Mine and Wall stocks (Figure 3; Webster and Pattison, 2013). This implies that the crust in this area was being eroded or tectonically unroofed during the Middle Jurassic. The granitoid and its surrounding contact aureole were unaffected by subsequent deformation and regional metamorphism (Webster and Pattison, 2013).

The deformed Baldy pluton yielded a U-Pb zircon date of 117.5 ±1.3 Ma, interpreted as the crystallization age. This age is consistent with, and overlaps within, the uncertainty of the 117 +4/–1 Ma U-Pb (combined titanite and allanite) age of Leclair et al. (1993). Because the Baldy pluton contains the same deformation fabrics as those in the enveloping metamorphic rocks, the new date constrains the upper limit of penetrative deformation in the footwall of the Midge Creek fault to approximately 118 Ma (D_2/M_2 of Leclair et al., 1993 and Moynihan, 2012; Figure 3). The Baldy pluton crosscuts the band of deformed Barrovian metamorphism, implying that it postdates peak metamorphism (Figure 3).

The Midge Creek stock (MCS) is situated between the Nelson and Bayonne batholiths (Figure 2) and cuts the penetrative structures and regional metamorphic isograds at the northern end of the Baldy pluton. It is undeformed, except at its northern tip, where the dominant foliation parallels the regional trend (Leclair, 1988). Leclair et al. (1993) interpreted the crystallization age of the MCS to be 111 ±4 Ma (mid-Cretaceous) from U-Pb (allanite) analyses. If this interpretation is correct it indicates that the MCS was emplaced during the latest stages of regional metamorphism and deformation in the area, with peak conditions occurring prior to 111 Ma. Combined with the work of Moynihan and Pattison (2013) to the north, and the new 118 Ma age of the deformed Baldy pluton, the age of deformation and regional metamorphism is constrained to the interval 143–111 Ma (Figure 3).

The postkinematic Summit stock yielded a U-Pb zircon date of 111.8 ±0.8 Ma, which is interpreted to be the age of crystallization. The similar mineralogy and age of both the Midge Creek stock and Summit stock confirm they are part of the Bayonne magmatic suite. Low pressure (staurolite free) andalusite-bearing contact aureoles, adjacent to both the Summit stock and the MCS, imply that they were emplaced at 7–11 km (Webster and Pattison, 2013; Figure 3). Biotite and hornblende K-Ar cooling ages for these stocks (102 and 109 Ma, respectively) are only several million years younger than the crystallization ages, implying that they crystallized, cooled and remained at a temperature below ~300°C, (i.e., at shallow depth), following their emplacement (Archibald et al., 1984).

The new U-Pb zircon age of 101.7 ±2.2 Ma for the crystallization age of the Emerald stock is also the timing of mineralization. Drillhole results and underground mine workings show that the Dodger and Emerald stocks are connected at depth, and are therefore of the same age (Lawrence, 1997). The new U-Pb age is in agreement with a K-Ar biotite age of 100 ±3 Ma from the Dodger stock (Dandy, 1997). These two results are within error of each other, implying that the mineralizing system and intrusion quickly cooled to below ~300°C following crystallization.

The new age of 108.8 ±1.2 Ma for the Mount Skelly pluton, combined with existing ages, requires a reinterpretation of the Bayonne batholith. The intrusive rocks that comprise the Bayonne batholith crystallized over an extended period of time, ca. 30 m.y. The plutons have different compositions, structural histories and varying depths of emplacement, confirming the Bayonne batholith is a composite body.

The cordierite-andalusite contact aureole around the Mount Skelly pluton is hosted in regionally metamorphosed lower-greenschist–facies Belt-Purcell Supergroup rocks in the hangingwall of the Purcell Trench fault (Webster and Pattison, 2013). The intrusion and surrounding strata in the hangingwall of the Purcell Trench fault are characterized by older K-Ar and Ar-Ar cooling ages (99–70 Ma) than the rocks in the footwall of the fault (60–46 Ma; Archibald et al., 1984). Based on the new U-Pb date, thermochronology and pressure and temperature estimates of contact metamorphism of the Mount Skelly contact aureole, the intrusion remained below 300°C after crystallization (i.e., at 7–11 km or higher in the crust). This contrasts with the geological history in the footwall of the Purcell Trench fault, south of the Bayonne batholith. Following the crystallization of the Mount Skelly pluton at 7–11 km in the crust, the rocks in the footwall of the PTF were later buried (ca. 80 Ma) to approximately 20 km, undergoing deformation and middle-amphibolite–facies metamorphism (Webster and Pattison, 2013).

Acknowledgments

This work was funded by a 2011 Geoscience BC grant to D.R.M. Pattison and E.R. Webster (1022684) and by Natu-

ral Sciences and Engineering Research Council (NSERC) Discovery Grant 037233 to D.R.M. Pattison. Insightful reviews provided by D.A. Archibald, D.P. Moynihan, A.L. Clifford, B. Hamilton and P. Starr improved this paper. Thanks to A. Dufrane for his assistance with LA-MC-ICP-MS analyses and C. Debuhr for his help on the SEM. Thanks also to J. Bjornson and C. Richardson for their excellent field assistance, and to W. Matthews for additional help.

References

Archibald, D.A., Glover, J.K., Price, R.A., Farrar, E. and Carmichael, D.M. (1983): Geochronology and tectonic implications of magmatism and metamorphism, southern Kootenay Arc and neighbouring regions, southeastern British Columbia, part 1: Jurassic to mid-Cretaceous; Canadian Journal of Earth Sciences, v. 20, no. 12, p. 1891–1913.

Archibald, D.A., Krogh, T.E., Armstrong, R.L. and Farrar, E. (1984): Geochronology and tectonic implications of magmatism and metamorphism, southern Kootenay Arc and neighbouring regions, southeastern British Columbia, part 2: mid-Cretaceous to Eocene; Canadian Journal of Earth Sciences, v. 21, no. 5, p. 567–583.

Bjornson, J. (2012): Contact metamorphism around the Lost Creek pluton and Summit Creek stock in the Summit Creek map area, southeastern British Columbia; B.Sc. thesis, University of Calgary, 66 p.

Brown, D.A., Doughty, T.P., Glover, J.K., Archibald, D.A., David, D.W. and Pattison, D.R.M. (1999): Field trip guide and road log: Purcell Anticlinorium to the Kootenay Arc, southeastern British Columbia, Highway 3—Creston to Summit Pass and northern Priest River Complex, west of Creston; BC Ministry of Energy and Mines, BC Geological Survey, Information Circular 1999-2.

Brown, D.A., Doughty, T.P. and Stinson, P. (1995): Geology and mineral occurrences of the Creston map area (82F/2); BC Ministry of Energy and Mines, BC Geological Survey, Open File 1995-15, 2 p., 1 map at 1:50 000 scale, URL <http://www.empr.gov.bc.ca/Mining/Geoscience/PublicationsCatalogue/OpenFiles/1995/Documents/OF1995-15.pdf> [November 25, 2013].

Dandy, L. (1997): Geological, geochemical and diamond drill report on the Jersey-Emerald property; BC Ministry of Energy and Mines, Assessment Report 24 910, 57 p.

Davis, D. (1995): Report on the U-Pb geochronology of rocks from the Priest River Complex, southeastern British Columbia; Royal Ontario Museum, Geology Department, unpublished report.

Devlin, W.J. and Bond, C.G. (1988): The initiation of the early Paleozoic Cordilleran miogeocline: evidence from the uppermost Proterozoic–Lower Cambrian Hamill Group of southeastern British Columbia; Canadian Journal of Earth Sciences, v. 25, p. 1–19.

Doughty, P.T. and Price, R.A. (1999): Tectonic evolution of the Priest River Complex, northern Idaho and Washington: a reappraisal of the Newport fault with new insights on metamorphic core complex formation; Tectonics, v. 18, p. 375–393.

Doughty, P.T. and Price, R.A. (2000): Geology of the Purcell Trench rift valley and Sandpoint conglomerate: Eocene en échelon normal faulting and synrift sedimentation along the eastern flank of the Priest River metamorphic complex, northern Idaho; Geological Society of America Bulletin, v. 112, no. 9, p. 1356–1374.

Doughty, P.T., Brown, D.A. and Archibald, D.A. (1997): Metamorphism of the Creston map area, southeastern British Columbia (82F/2); BC Ministry of Energy and Mines, BC Geological Survey, Open File 1997-5, 14 p. and 1 map at 1:50 000 scale, URL <http://www.empr.gov.bc.ca/Mining/Geoscience/PublicationsCatalogue/OpenFiles/1997/Documents/OF1997-05.pdf> [November 25, 2013].

Einarsen, J.M. (1994): Structural geology of the Pend d'Oreille area and tectonic evolution of the southern Kootenay Arc; Ph.D. thesis, University of Calgary.

Evenchick, C.A., McMechan, M.E., McNicoll, V.L. and Carr, S.D. (2007): A synthesis of the Jurassic-Cretaceous tectonic evolution of the central and southeastern Canadian Cordillera: exploring links across the orogen; Geological Society of America Special Paper 433, p. 117–145.

Ghent, E.D., Nicholls, J., Simony, P.S., Sevigny, J. and Stout, M. (1991): Hornblende geobarometry of the Nelson Batholith, southeastern British Columbia: tectonic implications; Canadian Journal of Earth Sciences, v. 28, p. 1982–1991.

Ghosh, D.K. (1995a): U-Pb geochronology of Jurassic to early Tertiary granitic intrusives from the Nelson-Castlegar area, southeastern British Columbia, Canada; Canadian Journal of Earth Sciences, v. 32, no. 10, p. 1668–1680.

Ghosh, D.K. (1995b): Nd- Sr isotopic constraints on the interactions of the Intermontane Superterrane with the western edge of North America in the southern Canadian Cordillera; Canadian Journal of Earth Sciences, v. 32, no. 10, p. 1740–1758.

Ghosh, D.K. and Lambert, R.S.J. (1995): Nd-Sr isotope geochemistry and petrogenesis of Jurassic granitoid intrusives, southeast British Columbia, Canada; *in* Jurassic Magmatism and Tectonics of the North American Cordillera, D.M. Miller and C. Busby (ed.), Geological Society of America Special Paper 299, p. 141–157.

Giroux, G. and Grunenberg, P. (2009): Summary report and preliminary resource calculations for the east Emerald and Emerald mine tungsten zones Jersey-Emerald property, BC; Sultan Minerals Inc., 80 p., URL <http://www.sultanminerals.com/i/pdf/NI43-101_EmeraldMineTungsten.pdf> [November 25, 2013].

Glombick, P., Brown, D.A. and MacLeod, R.F., compilers (2010): Geology, Creston, British Columbia; Geological Survey of Canada, Open File 6152, scale 1:50 000, URL <ftp://ftp2.cits.rncan.gc.ca/pub/geott/ess_pubs/261/261631/gscof_6152_e_2010_mn01.pdf> [November 25, 2013], doi:10.4095/288925

Glover, J.K. (1978): Geology of the Summit Creek area, southern Kootenay Arc, British Columbia; Ph.D. thesis, Queen's University, 144 p.

Höy, T. and Dunne, P.E.K. (1998): Geological compilation of the Trail map area, southeastern British Columbia (082F/3, 4, 5, 6); BC Ministry of Energy and Mines, BC Geological Survey, Geoscience Map 1998-1, scale 1:100 000, URL <http://www.empr.gov.bc.ca/Mining/Geoscience/PublicationsCatalogue/Maps/GeoscienceMaps/Documents/GM1998-01_Trail.pdf> [November 25, 2013].

Lawrence, E.A. (1997): Diamond drilling report on the Jersey property, Nelson Mining Division, Salmo, BC; BC Ministry of Energy and Mines, Assessment Report 25 349, 39 p.

Leclair, A.D. (1988): Polyphase structural and metamorphic histories of the Midge Creek area, southeast British Columbia: implications for tectonic processes in the central Kootenay Arc; Ph.D. thesis, Queen's University, 264 p.

Leclair, A.D., Parrish, R.R. and Archibald, D.A. (1993): Evidence for Cretaceous deformation in the Kootenay Arc on U-Pb and $^{40}Ar/^{39}Ar$ dating, southeastern British Columbia; *in* Current Research, Part A, Geological Survey of Canada, Paper 93-1A, p. 207–220.

Little, H. W. (1960): Nelson map area, British Columbia; Geological Survey of Canada, Memoir 308.

Logan, J.M. (2001): Prospective areas for intrusion-related gold-quartz veins in southern British Columbia; in Geological Fieldwork 2000, BC Ministry of Energy and Mines, BC Geological Survey, Paper 2000-1, p. 231–252, URL <http://www.empr.gov.bc.ca/Mining/Geoscience/PublicationsCatalogue/Fieldwork/Documents/2000/Logan_p231-252.pdf> [December 2013].

Ludwig, K.R. (2003): User's manual for Isoplot 3.0: a geochronology toolkit for Microsoft® Excel®; Berkeley Geochronology Center, Berkeley, CA, Special Publication 4, 74 p.

McAllister, A.L. (1951): Ymir map-area, British Columbia; Geological Survey of Canada, Paper 51-4, 58 p.

Monger, J.W.H., Price, R.A. and Templeman-Kluit, D.J. (1982): Tectonic accretion and the origin of the two major metamorphic and plutonic welts in the Canadian Cordillera; Geology, v. 10, p. 70–75.

Moynihan, D.P. (2012): Metamorphism and deformation in the central Kootenay Arc, southeastern British Columbia; Ph.D. thesis, University of Calgary.

Moynihan, D.P. and Pattison, D.R.M. (2013): Barrovian metamorphism in the central Kootenay Arc, British Columbia: petrology and isograd geometry; Canadian Journal of Earth Sciences, v. 50, p. 769–794, doi:10.1139/cjes-2012-0083

Paradis, S., MacLeod, R.F. and Emperingham, R., compilers (2009): Bedrock geology, Salmo, British Columbia; Geological Survey of Canada, Open File 6048, scale 1:50 000, URL <ftp://ftp2.cits.rncan.gc.ca/pub/geott/ess_pubs/247/247443/of_6048.pdf> [November 25, 2013], doi:10.4095/247443

Pattison, D.R.M. and Vogl, J.J. (2005): Contrasting sequences of metapelitic mineral-assemblages in the aureole of the tilted Nelson Batholith, British Columbia: implications for phase equilibria and pressure determination in andalusite-sillimanite type settings; Canadian Mineralogist, v. 43, p. 51–88.

Price, R.A. (2000): The southern Canadian Rockies: evolution of a foreland fold and thrust belt; Geological Association of Canada–Mineralogical Association of Canada, Joint Annual Meeting (GeoCanada 2000), Field Trip Guidebook 13, 246 p.

Reesor, J.E. (1996): Geology, Kootenay Lake, British Columbia; Geological Survey of Canada, Map 1864A, scale 1:100 000, URL <ftp://ftp2.cits.rncan.gc.ca/pub/geott/ess_pubs/207/207805/gscmap-a_1864a_e_1996_mg01.pdf > [November 25, 2013], doi:10.4095/207805

Rhodes, B.P. and Hyndman, D.W. (1984): Kinematics of mylonites in the Priest River "metamorphic core complex", northern Idaho and northeastern Washington; Canadian Journal of Earth Sciences, v. 21, p. 1161–1170.

Simonetti, A., Heaman, L.M., Chacko, T. and Banerjee, N.R. (2006): In situ petrographic thin section U-Pb dating of zircon, monazite, and titanite using laser ablation-MC ICP-MS; International Journal of Mass Spectrometry, v. 253, p. 87–97.

Simonetti, A., Heaman, L.M., Hartlaub, R.P., Creaser, R.A., McHattie, T.G. and Böhm, C.O. (2005): U-Pb zircon dating by laser ablation-MC-ICP-MS using a new multiple ion counting faraday collector array; Journal of Analytical Atomic Spectrometry, v. 20, no. 8, p. 677–686.

Tera, F. and Wasserburg, G.J. (1972): U-Th-Pb systematics in three Apollo 14 basalts and the problem of initial Pb in lunar rocks; Earth and Planetary Science Letters, v. 14, no. 3, p. 281–304.

Unterschutz, J.L.E., Creaser, R.A., Erdmer, P., Thompson, R.I. and Daughtry, K.L. (2002): North American margin origin of Quesnel terrane strata in the southern Canadian Cordillera: inferences from geochemical and Nd isotopic characteristics of Triassic metasedimentary rocks; Geological Society of America Bulletin, v. 114, no. 4, p. 462–475.

Warren, M.J. (1997): Crustal extension and subsequent crustal thickening along the Cordilleran margin of ancestral North America, western Purcell Mountains, southeastern British Columbia; Ph.D. thesis, Queen's University, 361 p.

Webster, E.R. and Pattison, D.R.M. (2013): Metamorphism and structure of the southern Kootenay Arc and Purcell Anticlinorium, southeastern British Columbia (parts of NTS 082F/02, /03, /06, /07); *in* Geoscience BC Summary of Activities 2012, Geoscience BC, Report 2013-1, p. 103–118.

Wheeler, J.O. and McFeely, P. (1991): Tectonic assemblage map of the Canadian Cordillera and adjacent parts of the United States of America; Geological Survey of Canada, Map1712A, scale 1:2 000 000.